Processing of low-probability sounds by cortical neurons

Nachum Ulanovsky, Liora Las and Israel Nelken

Department of Physiology, Hebrew University, Hadassah Medical School, Box 12272, Jerusalem 91120, Israel
Correspondence should be addressed to I.N. (israel@md.huji.ac.il)

Published online 24 March 2003; doi:10.1038/nn1032

The ability to detect rare auditory events can be critical for survival. We report here that neurons in cat primary auditory cortex (A1) responded more strongly to a rarely presented sound than to the same sound when it was common. For the rare stimuli, we used both frequency and amplitude deviants. Moreover, some A1 neurons showed hyperacuity for frequency deviants—a frequency resolution one order of magnitude better than receptive field widths in A1. In contrast, auditory thalamic neurons were insensitive to the probability of frequency deviants. These phenomena resulted from stimulus-specific adaptation in A1, which may be a single-neuron correlate of an extensively studied cortical potential—mismatch negativity—that is evoked by rare sounds. Our results thus indicate that A1 neurons, in addition to processing the acoustic features of sounds, may also be involved in sensory memory and novelty detection.

Neuronal adaptation, the decline over time of neuronal responses during sensory stimulation, is ubiquitous in the brain. Adaptation contributes to cortical gain control[1], enhances stimulus discriminability[2] and maximizes information transmission by matching the coding strategy to stimulus statistics[3]. Studies in both visual and auditory sensory areas have shown that adaptation is often stimulus-specific[2,4–11]. For example, neurons in auditory cortex, after having been presented with a repetitive, single-frequency tone for several minutes, show a specific decrease in response to subsequent test tones near that frequency[8]. Similarly, neurons in visual cortex, presented with a high-contrast 'adapting' stimulus of a certain orientation, show decreased responses specifically near that orientation[2,6,7].

Studies of such stimulus-specific adaptation (SSA), in both visual and auditory modalities, usually use one of two experimental approaches. The first is a method that uses long adapting sequences followed later by test stimuli[4–8]. This approach does not mimic natural scenarios particularly well; in natural sounds, the common background (mimicked by the long adapting sequence) is often intermixed with rare events (mimicked by the test stimuli). Furthermore, the common background may itself be changing over time scales of seconds, requiring fast, online adaptation. The second approach addresses these concerns by using pairs of stimuli—an adapting stimulus followed by a test stimulus. By this method, it has been shown that in some cases SSA can occur rapidly[2,9,10].

Several lines of evidence suggest that, in fact, it is natural to interpret neuronal adaptation in terms of the statistics of the stimulus ensemble. First, visual neurons can adapt in real time to the statistical distribution of input stimuli, and this adaptation can serve to maximize information transmission; thus, neuronal adaptation is tightly linked to the notion of optimal neural coding[3]. Second, natural acoustic backgrounds are highly variable and change rapidly in a stochastic manner[12]. Therefore, an important step in mimicking a naturalistic soundscape scenario is to use probabilistic stimuli. Third, the sensitivity of the mammalian auditory system to stimulus statistics is exemplified by the mismatch negativity (MMN)[13–29], an auditory potential that is evoked by rare sounds, and its size depends on the probability of the rare sounds. The MMN has been localized to the auditory cortex in humans[13–15], monkeys[21], cats[18–20] and guinea pigs[27–29], and is preattentive, as it is present under anesthesia[19,27–29].

In the present study, we used probabilistic stimuli to study adaptation in the auditory system. Our data, collected from both cortex and thalamus, provide evidence for a novel form of SSA that is present in primary auditory cortex but is absent in the auditory thalamus. This form of SSA is rapid, shows very high frequency sensitivity (hyperacuity) and is strongly dependent on the statistical properties of the stimulus ensemble. Furthermore, this form of SSA shares a large number of properties with the MMN, and we therefore propose that it is a neural correlate of MMN.

Results

To demonstrate SSA in single neurons of cat primary auditory cortex (**Fig. 1a**), we used a block containing 800 identical pure-tone stimuli, randomly intermixed with 20 rarely occurring tones (10 repetitions each). All 1,000 tones had the same amplitude and duration. The 20 frequencies were used to assess the influence of the common 'adapting' stimulus on the neuron's frequency response curve (the number of spikes evoked by a pure tone stimulus as a function of tone frequency, at a fixed sound amplitude). A reduction in the responses was observed near the adapting frequency, together with facilitation at flanking frequencies, a facilitation that was shown in previous studies as well[6,8,9]. Thus, common sounds can elicit SSA.

Responses of A1 neurons in an oddball design

To study the specific effect of probability on SSA, two frequencies were used in an oddball design protocol: tones with a deviant

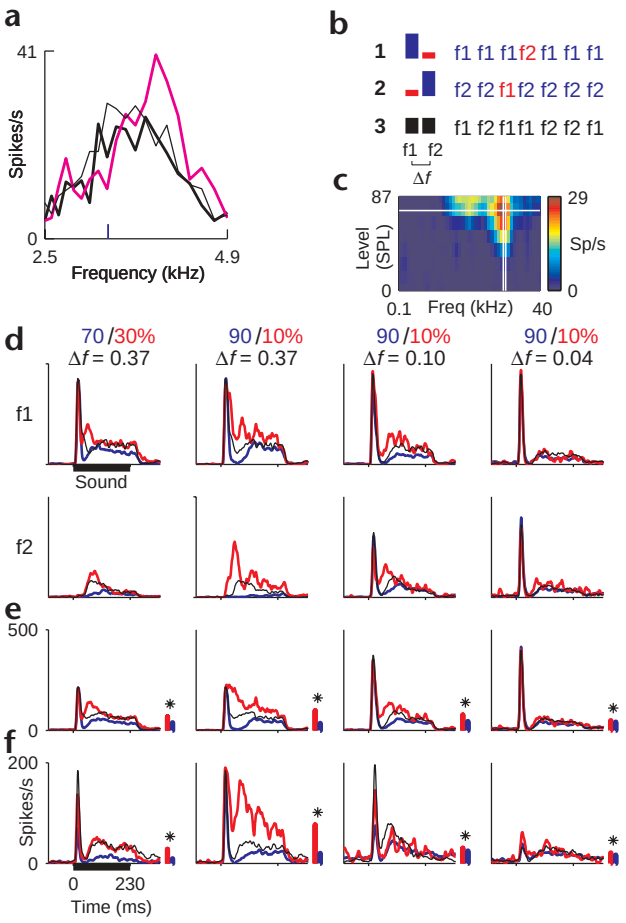

Fig. 1. Stimuli, and examples of single-neuron responses in A1. (**a**) Influence of stimulus-specific adaptation (SSA) on the frequency–response curve. Thick black line, before adaptation; magenta line, during adaptation; thin black line, after 30 s of recovery; blue tic mark on *x*-axis, adapting frequency (3.33 kHz). (**b**) The oddball stimuli. Each stimulus set consisted of three blocks (1–3). In block 1, the lower-frequency tone (f_1) was common ('standard') and the higher frequency tone (f_2) was rare ('deviant'). In block 2, the roles were reversed: f_2 was standard, and f_1 was deviant. In control block 3, f_1 and f_2 were mixed with 50/50% probability. (**c**) The receptive field of an A1 neuron, with white lines denoting the frequencies f_1 and f_2 (for $\Delta f = 0.10$) and the tone amplitude used in the oddball stimuli: these fall well inside the receptive field. (**d**) Responses (peri-stimulus time histogram, PSTH) of the neuron in **c** to the oddball stimuli. Shown are responses to the four stimulus sets (columns) and the two frequencies f_1 and f_2 (rows). Red lines, responses to deviant; blue lines, responses to standard; black lines, responses to control (50/50% probability). Each panel thus represents responses to the same physical stimulus in different probability contexts. (**e**) Responses of the same neuron, averaged over f_1 and f_2 separately for each probability condition. The small bars denote spike counts, and a star indicates significantly larger responses to the deviant than to the standard (*t*-test, one-tailed, $P < 0.0001$). Scales in **d** and **e** are identical. (**f**) Responses of another A1 neuron, presented as in **e**.

(rare) frequency were randomly embedded in blocks of tones at a standard (common) frequency (**Fig. 1b**). We manipulated both the probability of occurrence of the standard/deviant tones (90/10%, 70/30% and a control 50/50% case) and the normalized frequency difference (Δf) between the two tones ($\Delta f = 0.37$, 0.10, 0.04, defined as $\Delta f = (f_2 - f_1)/(f_2 \times f_1)^{1/2}$). The two frequencies were chosen to be in the vicinity of the best frequency of the neurons, and the amplitudes were relatively high, about 40 dB above minimal threshold (**Fig. 1c**). We used an interstimulus interval (ISI) of 736 ms (onset-to-onset), a tone duration of 230 ms and 400 trials per block. We recorded responses of single neurons in A1 and the medial geniculate body (MGB; the main thalamic auditory nucleus[30]) in seven halothane-anesthetized cats.

We measured the responses of A1 neurons to tones of the same frequency but with varying probability of occurrence (**Fig. 1d**). The responses were strongest to a tone when it was the deviant (red), and weakest when it was the standard (blue). Responses in the equiprobable control block (50/50% case, black) were intermediate. Thus, there was stronger neuronal adaptation to the standard than to the deviant. This differential adaptation was more prominent when Δf was larger (compare the three 90/10% cases, with varying Δfs) and when the deviant probability was smaller (compare the two $\Delta f = 0.37$ cases, with varying probabilities). To see this effect more clearly, we averaged the responses to the two frequencies for each probability condition separately (**Fig. 1e** and another neuron in **Fig. 1f**). For both neurons, the response to the same physical stimulus was significantly stronger when it was deviant than when it was standard (*t*-test, $P < 0.0001$), even for the smallest frequency difference ($\Delta f = 0.04$). In addition to the stimulus-specific component of the adaptation (the difference between standard and deviant), there was also a generalized decrease in responses as Δf decreased.

We computed the mean population responses of A1 neurons, averaged separately for each probability condition (**Fig. 2a**), as well as the population difference signal (DS), the difference between responses to the deviant and the standard (DS = deviant – standard; **Fig. 2b**). The DS was significantly larger than zero (*t*-test, $P < 0.0001$ in all cases), and it varied systematically with Δf and probability: the mean DS magnitude was positively correlated with Δf (one-way ANOVA grouped by Δf: $F = 16.0$, $P < 10^{-6}$) (*post-hoc* *t*-tests: $\Delta f = 0.37$ versus 0.10, $t = 3.86$, d.f. = 204, $P < 0.0001$; $\Delta f = 0.10$ versus 0.04, $t = 2.29$, d.f. = 173, $P < 0.02$). The mean DS magnitude was negatively correlated with deviant probability (90/10% versus 70/30%: $t = 1.68$, d.f. = 127, $P < 0.05$). The latency of the DS (**Fig. 2f**) was negatively correlated with Δf (one-way ANOVA grouped by Δf: $F = 7.39$, $P < 0.001$) (*post-hoc* *t*-tests: $\Delta f = 0.37$ versus 0.10, $t = 2.36$, d.f. = 203, $P < 0.01$; $\Delta f = 0.10$ versus 0.04, $t = 1.67$, d.f. = 171, $P < 0.05$). Moreover, for small Δf, the latency of the DS was longer than the latency of the response to the standard ($\Delta f = 0.37$: $t = 0.18$, d.f. = 98, n.s.; $\Delta f = 0.10$: $t = 1.87$, d.f. = 105, $P < 0.05$; $\Delta f = 0.04$: $t = 2.76$, d.f. = 66, $P < 0.005$), so that SSA was more prominent for sustained responses than for onset responses of A1 neurons. This extra delay of DS suggests that intracortical processing contributes to SSA.

As the mean population response is sensitive to the presence of neurons with high firing rates, we defined normalized stimulus-specific adaptation indices (SI) for each neuron separately. The frequency-specific index $SI(f_i)$, where $i = 1$ or 2, was defined for each frequency f_i as $SI(f_i) = [d(f_i) - s(f_i)]/[d(f_i) + s(f_i)]$ where $d(f_i)$ and $s(f_i)$ are responses to frequency f_i when it was deviant and standard, respectively. The neuron-specific SI was defined as $[d(f_1) + d(f_2) - s(f_1) - s(f_2)]/[d(f_1) + d(f_2) + s(f_1) + s(f_2)]$. Positive SI implies stronger response to the deviant than to the standard, and indeed the median neuron-specific SI (**Fig. 2c**) was significantly larger than zero for all four stimulus conditions (Sign test, $P < 0.05$, $P < 10^{-14}$, $P < 10^{-6}$, $P < 0.0002$, respectively, for the four columns of **Fig. 2**).

The frequency-specific SI (**Fig. 2d**) behaved similarly: a significantly larger proportion of the data was above the diagonal (Sign test, $P < 0.02$, $P < 10^{-17}$, $P < 10^{-5}$, $P < 0.005$, respectively),

such that $SI(f_1) + SI(f_2) > 0$. That the majority of neurons were above the diagonal indicates that SSA is present at the population level (**Fig. 2e**). The left panel shows the effect of adaptation on the frequency response curve $g(f)$ of a hypothetical neuron. Adaptation that does not change the shape of the curve (stimulus-insensitive 'fatigue') depresses it to $\alpha g(f)$ if f_1 is the standard or to $\beta g(f)$ if f_2 is the standard, with $1 > \alpha > \beta$ due to the higher firing rate in the latter case. Addition of SSA causes a specific dip around the adapting frequency (thin lines) and shifts the adaptation indices for this cell from the diagonal of the $SI(f_2)$-versus-$SI(f_1)$ plot (**Fig. 2e**, right panel) to a location above the diagonal. Note that, as shown in this example, the presence of SSA does not necessarily lead to a location in the upper right quadrant of the plot: this depends on the position of the two frequencies in relation to the shape of the frequency response curve. However, SSA necessarily leads to a location above the diagonal, as shown by the following calculation. By definition, $SI(f_1) = [d(f_1) - s(f_1)]/[d(f_1) + s(f_1)]$, so for stimulus-insensitive adaptation we can substitute as follows: $SI_{noSSA}(f_1) = [(\beta - \alpha)\, g(f_1)] / [(\beta + \alpha)\, g(f_1)] = (\beta - \alpha)/(\beta + \alpha)$. And similarly, $SI_{noSSA}(f_2) = [(\alpha - \beta)\, g(f_2)]/[(\alpha + \beta)\, g(f_2)] = (\alpha - \beta)/(\alpha + \beta)$. Summing the two, we obtain $SI_{noSSA}(f_1) + SI_{noSSA}(f_2) = 0$, which is the diagonal on the plot of $SI(f_2)$ versus $SI(f_1)$. Addition of SSA increases the differences between the two curves, yielding $SI_{SSA}(f_1)$ and $SI_{SSA}(f_2)$ such that $SI_{SSA}(f_1) > SI_{noSSA}(f_1)$ and $SI_{SSA}(f_2) > SI_{noSSA}(f_2)$. Therefore when SSA is present, $SI_{SSA}(f_1) + SI_{SSA}(f_2) > 0$, which are locations above the diagonal.

To study the dynamics of SSA, we computed the average population spike count versus trial number for the 90/10% probability, $\Delta f = 0.37$ (**Fig. 2g**). The initial responses to the standard and deviant stimuli were similar because the average was taken over identical frequency sets. However, the response to the standard underwent a fast and substantial adaptation (decreased by a factor of 1.54 after the very first trial), whereas the response to the deviant did not adapt.

The effects of stimulus probability described here could perhaps be explained by a simple model in which the responses at each trial are affected only by the immediately preceding stimulus, and the accumulation of such single-trial effects creates the observed time course. We tested such a model, and found that the data was not explained satisfactorily on the basis of the immediately preceding stimulus (data not shown).

To further study the influence of context on this SSA, we computed indices that compare for each neuron its frequency response curve with the responses to the standard and deviant tones from the oddball blocks, for all three Δf values at the 90/10% probability (**Fig. 2h**; Methods). Note that a deviant tone in the oddball blocks is presented within a context of a repetitive standard tone, whereas this same deviant tone in the frequency response curve (where it appears with a probability of 5%) is presented within a context of a large number of tones at different frequencies. For large Δf, the responses to a deviant tone were significantly stronger than the responses to a tone of the same frequency presented within the context of a large number of equiprobable tones (t-test for the six red points in **Fig. 2h**: $P < 0.01$, n.s., n.s., n.s., n.s. and $P < 0.01$, respectively). In contrast, there was no significant difference for standard tones for any of the frequencies. This result indicates again that a standard-deviant mixture can elicit SSA.

Frequency resolution by A1 neurons

Our results suggest that SSA may improve the capacity of neurons to discriminate between tones of slightly different frequencies in a probability-dependent manner. To test this possibility, we estimated the degree to which neurons could dis-

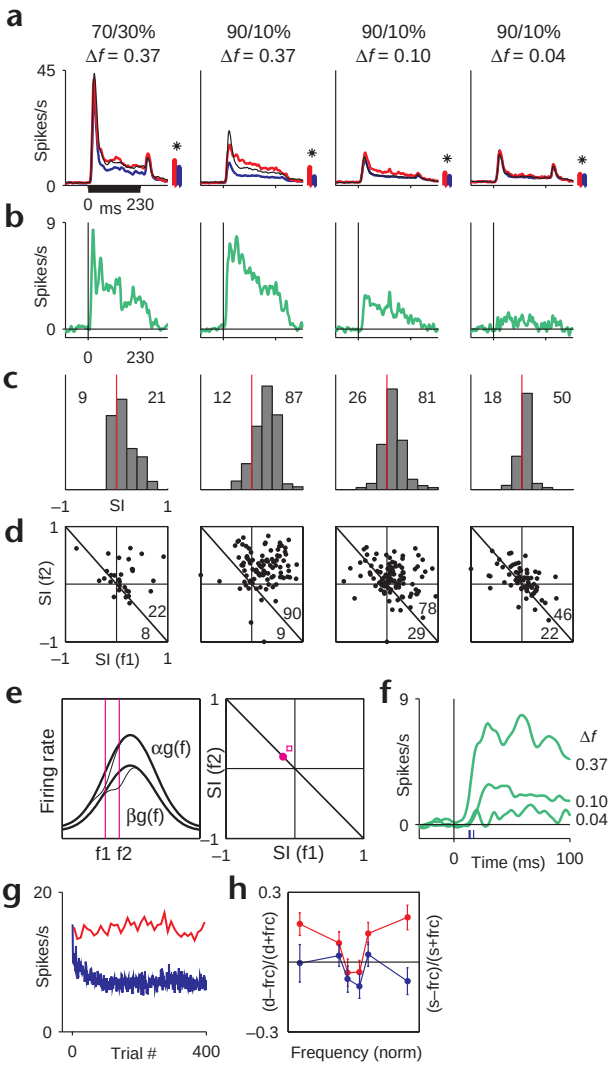

Fig. 2. Population analysis for A1 neurons. (**a**) Population PSTHs. (**b**) The difference signal (DS) between the population PSTHs for deviant and standard: DS = deviant –standard. (**c**) Histogram of the neuron-specific SI for all neurons. The number of neurons with SI > 0 (deviant stronger than standard on average) and SI < 0 is shown. (**d**) Scatterplot of $SI(f_2)$ versus $SI(f_1)$ for all neurons, with the number of dots above and below the diagonal. (**e**) Left, schematic frequency response curve of a hypothetical neuron, undergoing either stimulus-insensitive adaptation ('fatigue', thick lines) or SSA (thin lines). Right, plot of $SI(f_2)$ versus $SI(f_1)$ for stimulus-insensitive adaptation (filled circle) and for SSA (open square). (**f**) A high-resolution plot of the initial portion of DS, showing DS dependence on Δf (for 90/10%). Blue ticks are latency of the population response to the standard (12, 13 and 16 ms for Δf = 0.37, 0.10 and 0.04, respectively). (**g**) Time course of adaptation for the standard and deviant stimuli: average population spike count versus serial trial number, for 90/10%, Δf = 0.37. (**h**) Population comparison of the frequency response curve with the responses to the deviant (red) and to the standard (blue); see Methods. The six frequencies represent the three Δf values, in pairs (for example, Δf = 0.37 for two outermost points). Error bars, population mean ± s.e.m. The number of neurons here was smaller than in **c**, as only neurons that had frequency response curve data were included here.

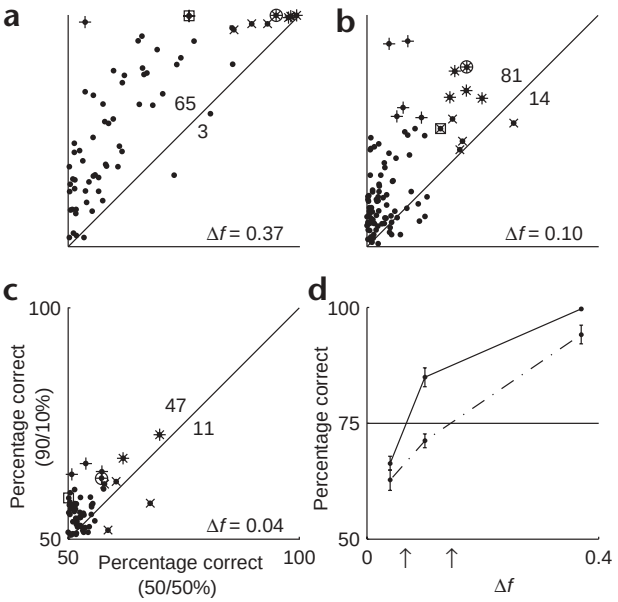

Fig. 3. Discriminability of frequency by A1 neurons, expressed as percentage correct. (**a**–**c**) Scatterplots of the discriminability, 90/10% versus 50/50%, for Δf = 0.37, 0.10 and 0.04. Each dot represents one neuron, and the number of dots above and below the diagonal are shown. Dots above the diagonal mean better discriminability for the 90/10% condition than for 50/50%. The total number of neurons is smaller than in **Fig. 2c** because only neurons that had 50/50% data were included here. The populations of the most sensitive neurons (top 10%), which differ in size and composition for the three Δf values, are marked for 90/10% (+) and for 50/50% (×). Stars (*) denote neurons that are most sensitive for both 90/10% and 50/50% conditions. The circle and square represent the two cells in **Fig. 1e** and **f**, respectively. (**d**) Psychometric curves, showing discriminability by the population of most sensitive neurons (mean ± s.e.m.). Solid line, 90/10%; hatched line, 50/50%; arrows, crossing points of 75% threshold.

criminate between frequencies f_1 and f_2 under different adaptation conditions. Discriminability was expressed as the estimated percent correct identification of frequency by each neuron using single-trial spike counts, computed using a standard technique from signal detection theory (Methods). The discriminability of rare versus common sounds (90/10%) was significantly better than that of equiprobable sounds (50/50%) for all Δf values, even for the smallest Δf (**Fig. 3a–c**; Sign test, $P < 10^{-15}$, $P < 10^{-11}$ and $P < 10^{-5}$ for $\Delta f = 0.37$, 0.10 and 0.04, respectively). For each Δf value and each probability condition separately, we selected for further analysis the population of most sensitive neurons (10% of neurons with highest discriminability). For $\Delta f = 0.37$, the frequency discriminability by these neurons improved from 94% (for the 50/50% probability condition) to 100% (for 90/10% probability) on average (*t*-test, $P < 0.02$). For $\Delta f = 0.10$, it improved from 71% to 85% (*t*-test, $P < 10^{-4}$), and for $\Delta f = 0.04$, it improved from 63% to 66% (*t*-test, n.s). The psychometric curves that summarize these results (**Fig. 3d**) cross the discriminability threshold (75% correct discrimination) at $\Delta f = 0.068 \pm 0.006$ for the 90/10% probability condition and at $\Delta f = 0.145 \pm 0.018$ for the 50/50% probability condition. The point of crossing defines the frequency resolution by these neurons. Thus, the population of most sensitive neurons improved its frequency resolution by a factor of 2.1 when exposed to rare sounds as opposed to equiprobable ones.

Additional properties of cortical SSA

After we identified this SSA for frequency deviants that is sensitive to stimulus statistics and has a very high-frequency resolution, two more questions arose. What is the temporal window of this SSA? Can this SSA be elicited by other acoustic parameters?

To further study the time course of SSA, we varied the interstimulus interval (ISI) between 375 and 4,000 ms (**Fig. 4a**) for 90/10% probability and $\Delta f = 0.10$. Results from well-separated single units and from multiunit clusters were reasonably similar. SSA decreased for long ISIs, and the DS was significantly larger than zero only at ISIs of 375 and 1,000 ms (*t*-test for DS > 0: $P < 10^{-15}$, $P < 10^{-6}$, n.s., n.s., respectively, for ISIs of 375, 1,000, 2,000 and 4,000 ms). In contrast, the number of multiunit clusters with SI(f_1) + SI(f_2) > 0 was still significantly larger than expected even at an ISI of 2,000 ms (Sign test, $P < 10^{-5}$, $P < 0.001$, $P < 0.01$, n.s, respectively, for the four ISIs). Neither test was significant at the 4,000-ms ISI. This temporal window raises the possibility that depressing synapses[31] whose longest time course of recovery is about 1,500 ms[31] may contribute to this form of SSA.

To study SSA for other acoustic parameters, we collected data for deviants and standards that differed by amplitude rather than by frequency (**Fig. 4b** and **c**). We presented a block in which the strong tone was the standard and the weak tone was the deviant, and another block where their roles were reversed (90/10%, amplitude difference of 16 dB, mean amplitude ~40 dB above minimal threshold). SSA was clearly present (*t*-test for DS > 0: $P < 10^{-13}$; Sign test for SI(Amp_1) + SI(Amp_2) > 0 (multiunits): $P < 0.001$). Thus, SSA in primary auditory cortex can be elicited by amplitude deviants, in addition to frequency deviants.

Responses of thalamic neurons

To test a possible subcortical origin of this SSA, we recorded from neurons in MGB using frequency deviants (90/10%, $\Delta f = 0.10$ condition). Individual MGB neurons showed very little SSA (**Fig. 5a** and **b**). The mean SI was not significantly different from zero (**Fig. 5c**; Sign test, n.s.), and the scatterplot of SI(f_2) versus SI(f_1) was approximately equally distributed above and below the diagonal (**Fig. 5d**; Sign test, n.s). Thus, at a parameter range in which SSA is very prominent in auditory cortex, SSA was not present in the thalamus. Therefore, this form of SSA seems to be generated at the level of the thalamocortical synapse or higher.

Discussion

In this work, we studied adaptation to probabilistic stimuli in the auditory system. We identified a form of adaptation that is present in single neurons in A1 but not in the MGB: it is stimulus-specific, very rapid (starts to develop within one trial), highly sensitive to stimulus statistics and has long latency, suggesting that intra-cortical processing contributes to this SSA. Such sensitivity to stimulus statistics is reported here for the first time in the auditory system, and we believe it may underlie auditory novelty detection.

SSA has previously been shown in various forms in the auditory system[8–11], but the specific form that we describe here differs in many respects. First, this SSA is cortical: we show that it is absent in the MGB, whereas previous studies indicate that some forms of SSA exist already at the level of the inferior colliculus (IC), the input station to the MGB[9,11]. This difference is probably due, in part, to the different stimulation protocol used: the IC studies[9,11] used either long tones without pauses between adapting and test stimuli (continuous frequency glides, ampli-

tude ramps or step instantaneous transitions were used) or tones with very short (100 ms) pauses. In such stimulation protocols, the test stimulus does not evoke much activity in A1: glide stimuli[9] usually elicit substantial responses in A1 only when the initial frequency is outside the neuron frequency area and the glide is toward the best frequency. In this case, a short burst may occur when the glide crosses the border of the frequency tuning curve[32], and it is impossible to assign a response to the final test frequency. In addition, tone pairs with short pauses are known to result in strong forward masking[33,34]. In either case, it is difficult to interpret the resulting activity patterns in A1 purely in terms of SSA. In the present study, SSA was shown for inter-tone pauses longer than 1,700 ms (ISI of 2,000 ms), much longer than the effects of forward masking in A1[33,34]. In fact, we believe that the differences between our results and the IC studies suggest the existence of two distinct mechanisms of SSA.

A second characteristic of the SSA shown here is its fast time course. In previous studies that also used long pauses[8], SSA developed over the course of minutes, whereas we found here SSA that develops within seconds. These differences in time course may be related to the finding from the visual system that the time course of adaptation scales with the time course of the stimulus[3].

The present form of SSA also has exquisite frequency resolution: it develops even for adapting stimuli that are extremely close to the test stimuli (for example, $\Delta f = 0.04$). In previous studies of SSA, such sensitivity was either not tested[9,11] or was tested mostly in multiunit clusters rather than in single neurons[8].

We interpret the results of this and previous studies as suggesting the existence of at least two distinct forms of SSA. One form of SSA is present at subcortical stations (most notably in paralemniscal 'belt' areas, such as ICx)[9], probably has relatively coarse stimulus specificity and requires continuous stimulus presentation or very short time gaps between stimuli. The other form of SSA, shown here, appears only at the cortical level, has a long latency concordant with cortical processing, and has a long memory (present for interstimulus gaps >1,700 ms). In addition, this form of SSA has very high stimulus specificity.

A neuronal correlate of mismatch negativity

This form of SSA in A1 neurons strongly resembles an important component of auditory event-related potentials (ERPs), the mismatch negativity (MMN)[13–29]. MMN has been extensively studied in relation to novelty detection[13] and sensory memory[13–16], and under various clinical conditions such as schizophrenia[24], dyslexia[25] and neglect[26]. Although MMN is one of the most widely studied cortical ERPs, we are not aware of any report on a single-neuron correlate of MMN.

MMN is measured in an oddball design protocol, and is defined as the difference between the ERPs for the deviant and the standard. MMN is thus similar to the DS described here (**Fig. 2b**). Additional similarities are that the main cortical generator of MMN is localized to the vicinity of the auditory cortex in humans[13–15], monkeys[21] and cats[18–20]. Moreover, MMN cannot be abolished by manipulating attention[13]; it exists in sleeping cats and in cats under deep anesthesia[18,19], as well as in anesthetized guinea pigs[27–29] and even in humans with coma[23]. Thus, MMN is truly preattentive[13]. As MMN has previously been shown to exist under the deep anesthetic pentobarbital in cats[19]

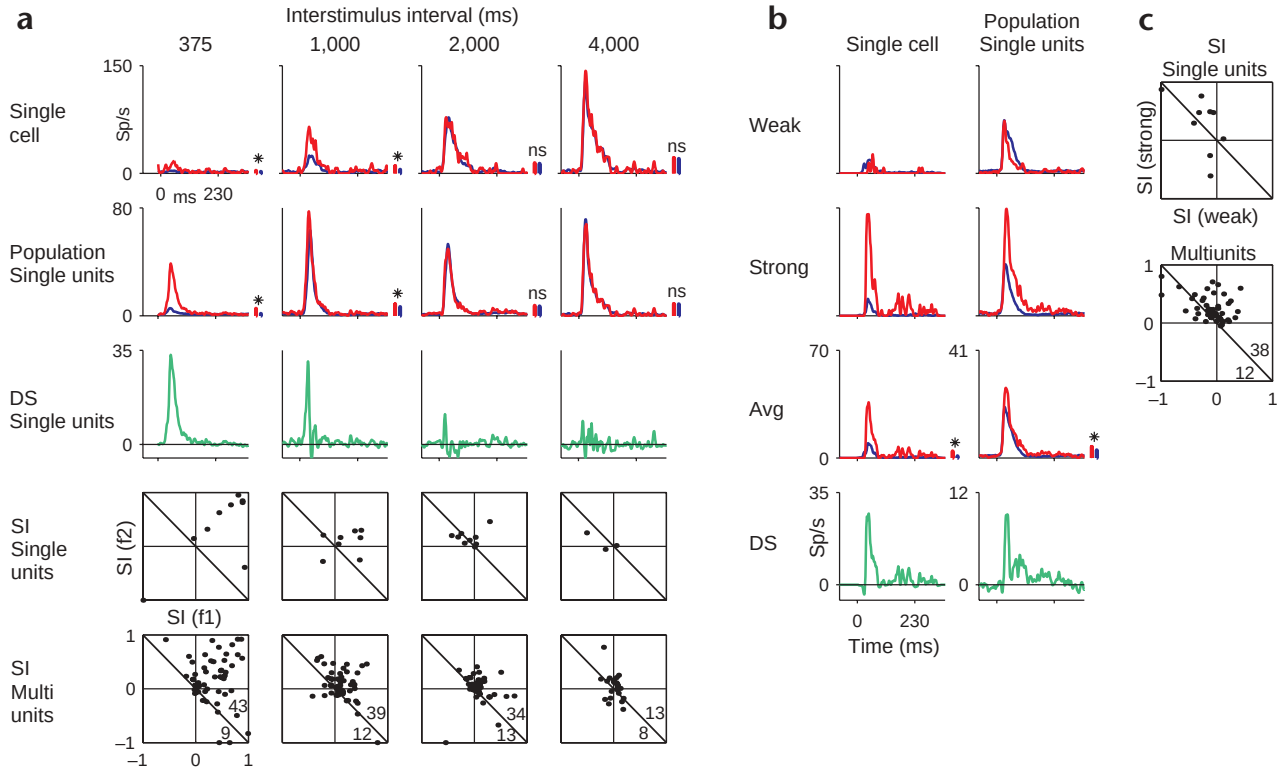

Fig. 4. Additional properties of cortical SSA. (**a**) Manipulating the interstimulus interval. Each column represents a different interstimulus interval; all rows show single-unit data, except the last row, which shows data recorded from multiunit clusters. (**b**–**c**) SSA for amplitude deviants. (**b**) Neuronal responses. The first row shows responses to the weak tone when it was deviant (red) and standard (blue); the second row shows responses to the strong tone, and the third row shows their average. (**c**) Scatterplots of SI(f_2) versus SI(f_1), for single-unit and multi-unit data. In both **a** and **b**, stars indicate significantly larger responses to the deviant than to the standard (*t*-test, one-tailed, $P < 0.05$).

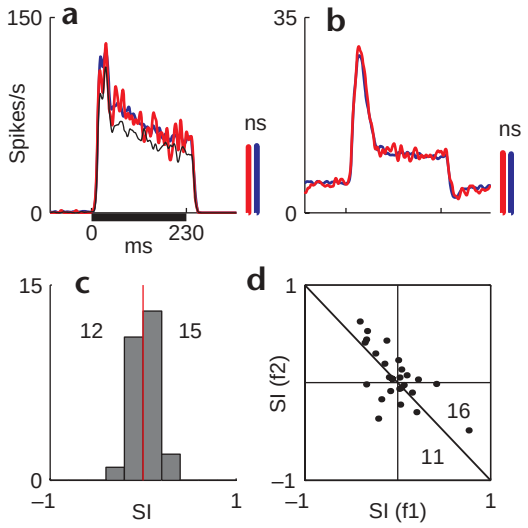

Fig. 5. Responses of neurons in the auditory thalamus (MGB) do not show SSA for 90/10%, Δf = 0.10. (**a**) PSTH of a single MGB neuron. (**b**) Population PSTH. (**c**) Histogram of neuron-specific SIs. (**d**) Scatterplot of SI(f_2) versus SI(f_1).

and under ketamine in guinea pigs[27–29], we could safely assume the existence of MMN under the rather light halothane anesthesia used in the current study.

MMN and the difference signal (DS) studied here share many properties (**Fig. 2**). First, the magnitudes of MMN[13,14,18,22] and DS (**Fig. 2b** and **f**) are both positively correlated with Δf but negatively correlated with the probability of deviant. Second, both MMN[16] and DS (**Fig. 2h**) exist when comparing the responses to a deviant tone in a block containing a single standard, with responses to the same tone in a block containing many equiprobable tones. This latter property is considered an important control for MMN[16]. The temporal dynamics of MMN and DS are also similar: (i) the latencies of both MMN[13,14,22] and DS (**Fig. 2f**) are negatively correlated with Δf, (ii) for small Δf, both MMN[13,15] and DS (**Fig. 2f**) have a longer latency than the responses to the standard, (iii) the magnitude of both MMN[13] and DS (**Fig. 2g**, the difference of the curves) is zero initially but increases with trial number, and (iv) the magnitude of both MMN[13] and DS (**Fig. 4a**) decreases for long ISIs. Finally, both MMN[13] and DS (**Fig. 4b**) exist for amplitude deviants.

The idea that neuronal adaptation may account for MMN has been raised previously[13,22], and our results provide the first direct evidence that neuronal adaptation has the right properties to account for MMN. Our comparison between MMN and DS suggests that a specific kind of adaptation, namely SSA in single auditory cortex neurons, may underlie cortical MMN.

MMN is not limited to frequency and amplitude deviants or to an A1 origin. It also exist for other kinds of deviants (such as location and duration)[13], and it is present in other auditory cortex fields[20,28,29], such as A2[20], and may perhaps even be stronger there than in A1[20,28,29]. We therefore predict that a similar form of SSA should be present in other auditory cortex fields and for other kinds of deviants, and that this SSA should behave similarly to MMN. This prediction remains to be tested, but some supporting evidence already exists: a form of SSA has been found in auditory cortex for interaural phase disparity[10], which is a cue for auditory localization. In addition, a form of SSA has been shown in both of the two major tonotopic fields of guinea pig auditory cortex[8], although with a much longer time course than the SSA described here. In fact, we believe that MMN, as recorded by surface electrodes, is the sum of many SSA processes occurring throughout all auditory cortex fields.

A previous attempt to localize the distribution of MMN sources within the auditory system was done in a series of studies in the guinea pig[27–29]. In these studies, local field potentials were recorded, and therefore MMN was measured directly. The conclusions of these studies were somewhat different from ours: MMN was found in paralemniscal belt regions of the MGB of guinea pigs, but not in its lemniscal core[27,29]. These studies also failed to identify MMN with epidural electrodes directly above A1 of guinea pigs, and concluded that MMN is a result of processing in the belt areas of the auditory forebrain[28,29].

The reasons for these differences are unclear. Species difference could play a role. Indeed, in contrast to the results in guinea pigs, MMN was shown (using intracortical[21] or epidural[18] electrodes) to exist within A1 of monkeys[21] and cats[18]; similar differences between guinea pigs and cats may occur in MGB. Differences in the stimulation parameters could also contribute. Another source of possible difference is the ketamine anesthesia used with the guinea pigs. In addition, the relationships between single-neuron events and evoked potentials are complex and not well understood. It could well be that the neural events leading to MMN in guinea pigs occur not only outside A1 but in A1 as well, but that because of geometrical and timing considerations, the evoked potential component appears only outside A1.

Most importantly, however, our single-neuron data positively show that neurons in A1 of cats are exquisitely sensitive to small changes in stimulus parameters in an oddball paradigm, and therefore the neural events that could give rise to MMN are probably present already in A1. Our results in MGB at the very least show that processing within A1 is centrally involved in SSA, and therefore presumably also in the generation of MMN.

Hyperacuity in single A1 neurons

An interesting aspect of the SSA shown here is that under oddball conditions (90/10% probability), the frequency resolution of neurons in A1 can be as small as $\Delta f = 0.068$, and moreover, stimulus probability affects discriminability even for $\Delta f = 0.04$ (**Fig. 3c**). This Δf is an order of magnitude smaller than the tuning width of A1 neurons, more than 90% of which have tuning width corresponding to $\Delta f > 0.7$ at the amplitude tested (D. Farkas and I.N., unpub. data). Moreover, this Δf is also an order of magnitude smaller than the tuning width of auditory peripheral neurons: in the auditory nerve, most fibers have tuning width corresponding to $\Delta f > 0.7$ at the amplitude tested, and about 90% of fibers have tuning width corresponding to $\Delta f > 0.4$ (ref. 35). These results constitute a form of neuronal hyperacuity. Psychophysical hyperacuity to frequency difference is well documented and is often explained by population averaging[36,37]. Indeed, hyperacuity has previously been shown at the level of neuronal populations (multiunit clusters)[8]. Here it is shown at the level of single neurons.

Psychophysical studies in humans show that the average frequency discrimination threshold is between 2% and 4% for normal untrained subjects[38,39], although highly trained subjects can discriminate frequencies down to ~0.5%. Psychophysical studies in cats[40] show average frequency discrimination thresholds of 2–10%. Thus, the most sensitive single neurons in our population responded at a similar sensitivity as trained cats and at nearly the same sensitivity as untrained humans.

In summary, we report four main findings here. First, audi-

tory cortex neurons respond more strongly to a rare sound than to the same sound when common, as a result of stimulus-specific adaptation (SSA). This was shown for both frequency and amplitude deviants, and we expect that the same will be true for other acoustic parameters. This form of SSA was extremely rapid and had high parameter sensitivity, as shown by its hyperacuity for frequency deviants. Second, frequency discrimination by auditory cortex neurons is better when processing deviant frequencies, as compared to equiprobable ones. We therefore predict that behavioral frequency discrimination by human or animal subjects should also be better for rare sounds. Third, the origin of this form of SSA for frequency deviants is above the thalamus, with a probable contribution of intracortical processing. We hypothesize a supra-thalamic origin of such SSA for other acoustic deviants, especially when the differences between the common and rare sounds are small. And fourth, we suggest that this SSA is a single-neuron correlate of an important cortical evoked potential, the MMN. In fact, this relationship between MMN (which is implicated in sensory memory) and SSA suggests that SSA in single cortical neurons may be a neuronal correlate of sensory memory. Thus, our results shed light on the relationships between single-neuron activity and cortical evoked potentials that are used to study higher brain functions.

Methods

Electrophysiology and stimulus presentation. Anesthesia was induced by ketamine and xylazine and maintained with halothane (0.25–1.25% as needed) using standard protocols authorized by the committee for animal care and ethics of the Hebrew University – Hadassah Medical School[12,41]. Anesthesia level was monitored by direct measurement of blood pressure (kept around 100 mmHg). During data acquisition, the halothane level could usually be maintained at its minimum, and the animals were sufficiently anesthetized so that they did not resist the respirator and did not have to be paralyzed. Single neurons were recorded using up to four glass-coated tungsten microelectrodes, and were spike-sorted either online (MSD, Alpha-Omega, Nazareth Illit, Israel: template-based sorting) or offline under manual control (in-house sorting program, using principal component analysis of spike shapes). Recordings were made in primary auditory cortex (A1, 5 cats), in auditory thalamus (MGB, 1 cat) and in A1 and MGB simultaneously (1 cat). Thalamic recordings were done in all major subdivisions of the MGB. Neurons were selected for analysis if they were well-separated, had significant auditory responses (t-test, $P < 0.05$) and had stable spontaneous firing rate. A total of 158 neurons from A1 and 27 neurons from MGB are analyzed here. The data for the dependence on ISI and the SSA for amplitude deviants (**Fig. 4**) consist of an additional set of 10 well-separated neurons and 52 multiunit clusters collected in one animal.

Stimuli were pure tones generated digitally (Tucker-Davis Technologies, Alachua, Florida: AP2), converted to analog (Tucker-Davis: DA3-4) and presented to the animal through sealed, calibrated earphones (designed by G. Sokolich). For the oddball stimuli, tone frequencies were chosen close to the best frequency of the neuron and were centered on a fixed value for each neuron, for all three Δfs (so that $(f_2 \times f_1)^{1/2}$ was held constant). Stimulus amplitude was relatively high (about 40 dB above minimal threshold) and was held constant for all the stimuli presented to a given neuron. The probability of appearance of standard/deviant and the frequency difference (Δf) were manipulated. The tone sequences in each block were generated as a random permutation of the total number of stimuli in the block. Although this precluded complete serial independence between successive choices of tone frequencies, the constraint of a fixed number of stimuli was important mostly toward the end of each block, whereas the effects that we describe are extremely fast and occur at the beginning of each block, where the serial independence approximation is good.

Δf was defined as $(f_2 - f_1)/(f_2 \times f_1)^{1/2}$. The following parameters were held constant for all neurons: number of tones per block (400), rise/fall times (a linear 10-ms ramp) and tone duration (230 ms). The main data were collected at an interstimulus interval (ISI)of 736 ms, onset-to-onset. To collect data on the influence of ISI (**Fig. 4a**), we varied those intervals and also used 200 tones per block for intervals of 1,000 ms and higher. Frequency–response curves (as in **Fig. 1a**) were measured using 20 frequencies spanning about 1 octave centered approximately at the same center frequency as the oddball stimuli. Each frequency was presented ten times in a pseudo-random order. The stimulus amplitude, rise/fall times, tone duration and interstimulus interval were identical to those used in the main experiment. The same stimulus parameters were used also for the experiment on amplitude deviants (**Fig. 4b** and **c**). For measuring the full frequency response areas of neurons (**Fig. 1c**), we used randomly presented tones, with 45 frequencies and 8 amplitudes.

Data analysis. Spike counts were measured in a window of 330 ms, starting at stimulus onset and ending 100 ms after stimulus offset. PSTHs were smoothed with a 10-ms Hamming window for display only, but analyses were done without smoothing. Population PSTHs (**Figs. 2a**, **4a** and **b**, **5b**) were computed as the 5% trimmed mean of single-neuron PSTHs, without prior normalization. An approximately equal number of neurons were tested with 70/30% probabilities and 65/35% probabilities: these data were pooled together. We defined normalized stimulus-specific adaptation indices (SI, **Fig. 2d**) for each frequency as $SI(f_i) = [d(f_i) - s(f_i)]/[d(f_i) + s(f_i)]$ ($i = 1,2$), where $d(f_i)$ and $s(f_i)$ are responses to frequency f_i when it was deviant and standard, respectively. The neuron-specific SI (**Fig. 2c**) was defined as $[d(f_1) + d(f_2) - s(f_1) - s(f_2)]/[d(f_1) + d(f_2) + s(f_1) + s(f_2)]$. For the time course of SSA (**Fig. 2g**), the responses to the 360 standard and 40 deviant trials were combined by their order of presentation in the sequence, and then plotted at their original (400 trials long) time scale. To compare the frequency response curves with the oddball data (**Fig. 2h**), we computed for each neuron normalized indices: $(d - frc)/(d + frc)$ for the deviant and $(s - frc)/(s + frc)$ for the standard, where d, s and frc are the spike counts for the deviant (d), standard (s) and the frequency response curve (frc) at the same frequency. The value of frc was computed at the exact frequencies of the oddball stimuli using cubic spline interpolation of the frequency response curve. The figure shows population averages of these data.

The latency of the difference signal (DS, **Fig. 2f**) was defined as the time when the DS crossed the following threshold: 0.3*Max(DS) + 2.5*std(DS(spontaneous)) (note that the DS baseline was around 0). The DS was smoothed with a three-point Hamming window before thresholding. The latency of the responses to the standard was similarly defined.

To compute the frequency discriminability by neurons (**Fig. 3**), we used the distributions of spike-count data of each neuron. For each frequency pair (f_1, f_2), we constructed a receiver operating characteristic (ROC) curve[42] based on the appropriate pair of spike-count distributions. The percentage of correct responses was computed as the area under the ROC curve[42]; this is the probability with which an ideal observer would identify the correct frequency on the basis of spike counts. For the y-axes (90/10% data, **Fig. 3a–c**), we took the larger of the two percentage values from the two blocks (**Fig. 1b**, blocks 1 and 2).

Statistical tests were considered significant when $P < 0.05$, except where multiple points were tested (**Fig. 2h**, we used $P < 0.01$).

Acknowledgments

We thank G. Morris and G. Chechik for critical reading of the manuscript, and G. Karmos, I. Winkler, L. Deouell, H. Pratt, S. Bentin, S. Marom and M. Ahissar for stimulating discussions on the SSA–MMN comparison. This work was supported by a Human Frontiers Science Program grant to I.N. and a Horowitz Foundation predoctoral fellowship to N.U.

Competing interests statement

The authors declare that they have no competing financial interests.

Received 23 December 2002; Accepted 13 February 2003

1. Ohzawa, I., Sclar, G. & Freeman, R.D. Contrast gain control in the cat visual cortex. *Nature* **298**, 266–268 (1982).
2. Müller, J.R., Metha, A.B., Krauskopf, J. & Lennie, P. Rapid adaptation in visual cortex to the structure of images. *Science* **285**, 1405–1408 (1999).

3. Fairhall, A.L., Lewen, G.D., Bialek, W. & de Ruyter Van Steveninck, R.R. Efficiency and ambiguity in an adaptive neural code. *Nature* **412**, 787–792 (2001).
4. Movshon, J.A. & Lennie, P. Pattern-selective adaptation in visual cortical neurones. *Nature* **278**, 850–852 (1979).
5. Saul, A.B. & Cynader, M.S. Adaptation in single units in visual cortex: the tuning of aftereffects in the spatial domain. *Vis. Neurosci.* **2**, 593–607 (1989).
6. Dragoi, V., Sharma, J. & Sur, M. Adaptation-induced plasticity of orientation tuning in adult visual cortex. *Neuron* **28**, 287–298 (2000).
7. Dragoi, V., Rivadulla, C. & Sur, M. Foci of orientation plasticity in visual cortex. *Nature* **411**, 80–86 (2001).
8. Condon, C.D. & Weinberger, N.M. Habituation produces frequency-specific plasticity of receptive fields in the auditory cortex. *Behav. Neurosci.* **105**, 416–430 (1991).
9. Malone, B.J. & Semple, M.N. Effects of auditory stimulus context on the representation of frequency in the gerbil inferior colliculus. *J. Neurophysiol.* **86**, 1113–1130 (2001).
10. Malone, B.J., Scott, B.H. & Semple, M.N. Context-dependent adaptive coding of interaural phase disparity in the auditory cortex of awake macaques. *J. Neurosci.* **22**, 4625–4638 (2002).
11. Sanes, D.H., Malone, B.J. & Semple, M.N. Role of synaptic inhibition in processing of dynamic binaural level stimuli. *J. Neurosci.* **18**, 794–803 (1998).
12. Nelken, I., Rotman, Y. & Bar-Yosef, O. Responses of auditory-cortex neurons to structural features of natural sounds. *Nature* **397**, 154–157 (1999).
13. Näätänen, R. *Attention and Brain Function* (Lawrence Erlbaum, Hillsdale, New Jersey, 1992).
14. Tiitinen, H., May, P., Reinikainen, K. & Näätänen, R. Attentive novelty detection in humans is governed by pre-attentive sensory memory. *Nature* **372**, 90–92 (1994).
15. Picton, T.W., Alain, C., Otten, L., Ritter, W. & Achim, A. Mismatch negativity: different water in the same river. *Audiol. Neurootol.* **5**, 111–139 (2000).
16. Jacobsen, T. & Schröger, E. Is there pre-attentive memory-based comparison of pitch? *Psychophysiology* **38**, 723–727 (2001).
17. Näätänen, R., Tervaniemi, M., Sussman, E., Paavilainen, P. & Winkler, I. "Primitive intelligence" in the auditory cortex. *Trends Neurosci.* **24**, 283–288 (2001).
18. Csépe, V., Karmos, G. & Molnár, M. Evoked potential correlates of stimulus deviance during wakefulness and sleep in cat—animal model of mismatch negativity. *Electroencephalogr. Clin. Neurophysiol.* **66**, 571–578 (1987).
19. Csépe, V., Molnár, M., Karmos, G. & Winkler, I. Effect of changes in stimulus frequency on auditory evoked potentials in awake and anaesthetized cats. in *Sleep 88* (eds. Horne, J. & Lovie, P.) 210–211 (Gustav Fischer, Stuttgart/New York, 1989).
20. Pincze, Z., Lakatos, P., Rajkai, C., Ulbert, I. & Karmos, G. Separation of mismatch negativity and the N1 wave in the auditory cortex of the cat: a topographic study. *Clin. Neurophysiol.* **112**, 778–784 (2001).
21. Javitt, D.C., Steinschneider, M., Schroeder, C.E., Vaughan, H.G. Jr. & Arezzo, J.C. Detection of stimulus deviance within primate primary auditory cortex: intracortical mechanisms of mismatch negativity (MMN) generation. *Brain Res.* **667**, 192–200 (1994).
22. May, P. *et al.* Frequency change detection in human auditory cortex. *J. Comput. Neurosci.* **6**, 99–120 (1999).
23. Fischer, C., Morlet, D. & Giard, M. Mismatch negativity and N100 in comatose patients. *Audiol. Neurootol.* **5**, 192–197 (2000).
24. Javitt, D.C. Intracortical mechanisms of mismatch negativity dysfunction in schizophrenia. *Audiol. Neurootol.* **5**, 207–215 (2000).
25. Kujala, T. & Näätänen, R. The mismatch negativity in evaluating central auditory dysfunction in dyslexia. *Neurosci. Biobehav. Rev.* **25**, 535–543 (2001).
26. Deouell, L.Y., Hamalainen, H. & Bentin, S. Unilateral neglect after right-hemisphere damage: contributions from event-related potentials. *Audiol. Neurootol.* **5**, 225–234 (2000).
27. Kraus, N. *et al.* Discrimination of speech-like contrasts in the auditory thalamus and cortex. *J. Acoust. Soc. Am.* **96**, 2758–2768 (1994).
28. King, C., McGee, T., Rubel, E.W., Nicol, T. & Kraus, N. Acoustic features and acoustic changes are represented by different central pathways. *Hear. Res.* **85**, 45–52 (1995).
29. Kraus, N., McGee, T., Littman, T., Nicol, T. & King, C. Nonprimary auditory thalamic representation of acoustic change. *J. Neurophysiol.* **72**, 1270–1277 (1994).
30. Andersen, R.A., Knight, P.L. & Merzenich, M.M. The thalamocortical and corticothalamic connections of AI, AII, and the anterior auditory field (AAF) in the cat: evidence for two largely segregated systems of connections. *J. Comp. Neurol.* **194**, 663–701 (1980).
31. Markram, H., Wang, Y. & Tsodyks, M. Differential signaling via the same axon of neocortical pyramidal neurons. *Proc. Natl. Acad. Sci. USA* **95**, 5323–5328 (1998).
32. Phillips, D.P., Mendelson, J.R., Cynader, M.S. & Douglas, R.M. Responses of single neurones in cat auditory cortex to time-varying stimuli: frequency-modulated tones of narrow excursion. *Exp. Brain. Res.* **58**, 443–454 (1985).
33. Calford, M.B. & Semple, M.N. Monaural inhibition in cat auditory cortex. *J. Neurophysiol.* **73**, 1876–1891 (1995).
34. Brosch, M. & Schreiner, C.E. Time course of forward masking tuning curves in cat primary auditory cortex. *J. Neurophysiol.* **77**, 923–943 (1997).
35. Liberman, M.C. Auditory-nerve response from cats raised in a low-noise chamber. *J. Acoust. Soc. Am.* **63**, 442–455 (1978).
36. Moore, B.C.J. Frequency analysis and pitch perception. in *Human Psychophysics* (eds. Yost, W.A., Popper, A.N. & Fay, R.R.) 56–115 (Springer, New York, 1993).
37. Delgutte, B. Physiological models for basic auditory percepts. in *Auditory Computation* (eds. Hawkins, H.L., McMullen, T.A., Popper, A.N. & Fay, R.R.) 157–220 (Springer, New York, 1996).
38. Amitay, S., Ahissar, M. & Nelken, I. Auditory processing deficits in reading disabled adults. *J. Assoc. Res. Otolaryngol.* **3**, 302–320 (2002).
39. Ahissar, M., Protopapas, A., Reid, M. & Merzenich, M.M. Auditory processing parallels reading abilities in adults. *Proc. Natl. Acad. Sci. USA* **97**, 6832–6837 (2000).
40. Masterton, R.B., Granger, E.M. & Glendenning, K.K. Psychoacoustical contribution of each lateral lemniscus. *Hear. Res.* **63**, 57–70 (1992).
41. Bar-Yosef, O., Rotman, Y. & Nelken, I. Responses of neurons in cat primary auditory cortex to bird chirps: effects of temporal and spectral context. *J. Neurosci.* **22**, 8619–8632 (2002).
42. Green, D.M. & Swets, J.A. *Signal Detection Theory and Psychophysics* (Wiley, New York, 1966).